Scattering of 22.5-MeV Protons from Zirconium and the Symmetry Term in the Nuclear Optical Potential

J. B. BALL, C. B. FULMER, AND R. H. BASSEL
Oak Ridge National Laboratory, Oak Ridge, Tennessee*
(Received 23 March 1964]

Differential cross sections for the elastic scattering of 22.5-MeV protons were measured from isotopically enriched foils of Zr^{90}, Zr^{91}, Zr^{92}, Zr^{94}, and Zr^{96} over an angular range of 20 to 150°. The ratio to the Rutherford cross section exhibits a smooth decrease in the angular position of the maxima and minima as the mass of the target nucleus is increased. The magnitude of these shifts of the maxima and minima is larger than expected on the basis of previously observed 22.2 -MeV proton elastic scattering on targets over a large range of A values. This larger shift in the angular position of the features is in agreement with a dependence of the real nuclear potential well depth on the nuclear symmetry parameter, $(N\text{-}Z)/A$. A detailed optical model fit to the data yields a real nuclear potential of the form, $-V=[43.4+27.8(N-Z)/A]$ MeV.

INTRODUCTION

IT has been suggested by Lane[1] that the real optical-model potential is of the form

$$U=U_0+(U_1/A)\mathbf{t}\cdot\mathbf{T}. \quad (1)$$

The $\mathbf{t}\cdot\mathbf{T}$ operator contains a term t_+T_- which can account for the "analog" states in the (p,n) reaction observed by Anderson *et al.*[2] For the elastic scattering of nucleons, the operator contains a term t_zT_z resulting in a nuclear symmetry term in the real optical potential of the form

$$V=V_0\pm V_1(N-Z)/A \quad (4)$$

for neutrons and protons, respectively. Thus, the elastic scattering of nucleons for medium weight nuclei provides another method of determining the magnitude of $U_1(=4V_1)$.

The elastic scattering of protons near 10 MeV from pairs of isobars[3,4] and from the two copper isotopes[5] has shown the presence of the nuclear symmetry term at these energies. Scattering from isobars at 22.2 MeV did not yield conclusive evidence for the need of a symmetry term at the higher energy.[6] This led to the conjecture that possibly the term was velocity-dependent. A survey by Perey[7] of the elastic scattering of protons with energies between 9 and 22 MeV from many nuclei showed that the magnitude of the symmetry term found at the lower energies was also consistent with the data at higher energy.

The difficulties experienced in extracting a consistent value of the symmetry term from scattering on isobars may well lie in the inability to establish a consistent set of parameters for the pair. Isobars not only possess a different nuclear charge but usually the two members of the pair have significantly different nuclear deformation parameters. Frequently the deformation parameters for conveniently available isotopes and isobaric pairs are rather large resulting in strong coupling between the elastic channel and inelastic channels.[8]

The scattering of protons from the zirconium isotopes offers two distinct advantages over scattering from isobars in determining the nuclear symmetry term. First, since the zirconium isotopes all possess the same nuclear charge, the Coulomb correction term to the proton potential well becomes a second-order effect. Second, since all of the nuclei possess a filled proton level and the isotopic sequence begins with a major closed neutron shell, the zirconium isotopes are expected to have small deformation parameters; consequently, the elastic scattering should not be significantly perturbed by coupling with collective states.

EXPERIMENTAL

The data were obtained with the external proton beam of the ORNL 86-in. cyclotron. The energy available during the course of this experiment was 22.5 MeV. The scattered protons were detected with a NaI(Tl) scintillation counter mounted on the continuously rotatable top of a 24-in. diam scattering chamber. The proton beam entered the chamber through a $\frac{1}{4}$-in.-diam collimator and after passing through the target was monitored by stopping in a Faraday cup. The detector aperture subtended an angle of about $\frac{1}{2}$ deg and the angular position of the counter could be read to within $\frac{1}{4}$ deg. The beam axis in the chamber was checked by left-right scattering and found to be centered within $\frac{1}{4}$ deg.

The target foils were rolled from isotopically enriched samples of zirconium; the isotopic composition of the targets is given in Table I.[9] The nominal thickness of

* Operated for USAEC by Union Carbide Corporation.
[1] A. M. Lane, Phys. Rev. Letters 8, 171 (1962); Nucl. Phys. 35, 676 (1962).
[2] J. C. Anderson, C. Wong, and J. W. McClure, Phys. Rev. 126, 2170 (1962).
[3] J. Benveniste, A. C. Mitchell, and C. B. Fulmer, Phys. Rev. 129, 2173 (1963).
[4] J. Benveniste, A. C. Mitchell, and C. B. Fulmer, Phys. Rev. 133, B317 (1964).
[5] J. Benveniste, R. Booth, and A. Mitchell, Phys. Rev. 123, 1818 (1961).
[6] C. B. Fulmer, Phys. Rev. 125, 631 (1962).
[7] F. G. Perey, Phys. Rev. 131, 745 (1963).
[8] B. Buck, Phys. Rev. 130, 712 (1963).
[9] The isotopic abundances were determined and the metallic foils were prepared by the Isotopes Division of this Laboratory.

TABLE I. Isotopic abundances of targets. Composition (%)

Target \ Contents	Zr^{90}	Zr^{91}	Zr^{92}	Zr^{94}	Zr^{96}
Zr^{90}	98.66	0.77	0.34	0.18	0.04
Zr^{91}	6.97	87.0	5.23	0.79	0.2
Zr^{92}	2.45	2.18	93.22	1.97	0.18
Zr^{94}	1.47	0.37	0.69	97.06	0.41
Zr^{96}	10.0	2.15	3.27	4.41	80.1

the foils was ~ 5 mg/cm^2 but the method of preparation did not result in uniform thickness. The actual thickness of the target areas exposed to the beam was determined by mapping the central areas of the foils by measurement of the energy loss of alpha particles from a natural source.

The data were taken at 10° intervals. Two passes were made to obtain data at 5° intervals from about 20 to 160°. At a later date, more points were measured near the maxima and minima observed from the initial runs to provide greater detail. The data for angles up to 120° were taken as transmission data and beyond 120° as reflection data. A typical spectrum from Zr^{92} is shown in Fig. 1. At some angles the inelastic scattering to the first 2+ state was partially obscured by a large elastic peak. Difficulties in separating these two peaks occurred only where the uncertainty in separation did not significantly affect the elastic-scattering cross sections. For Zr^{90} and Zr^{96} the experimental resolution was not sufficient to separate the 2+ and 3− states from each other, but the composite peak was clearly separated from the elastic peak. The usual detector resolution was about 450 keV (2%) for the full energy protons. Subsequent analysis of the scattered proton spectra from the Zr^{90} target with a high resolution magnetic analysis system showed a negligible contribution from oxygen and carbon impurities. No evidence for scattering from low mass impurities was seen for the counter data at large angles and it was assumed that all the targets were relatively free of oxygen and carbon contamination. The major contribution to the experimental uncertainties in the cross sections was the nonuniform thickness of the targets.

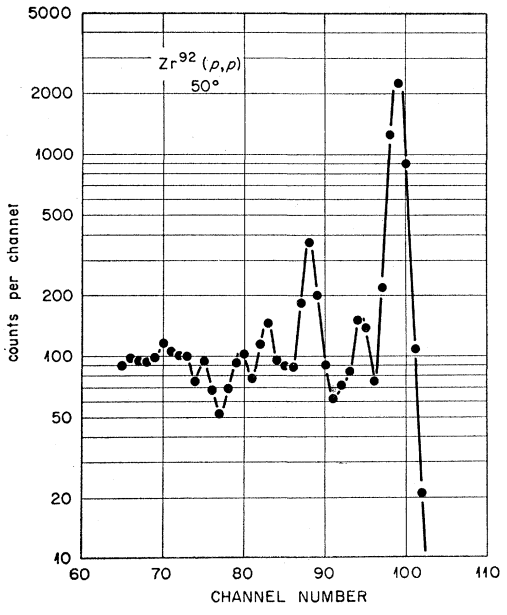

FIG. 1. Representative pulse-height spectrum. The peaks at channel numbers 99, 94, and 88 correspond to elastic scattering and inelastic scattering that excites the first 2+ state and the first 3− state, respectively.

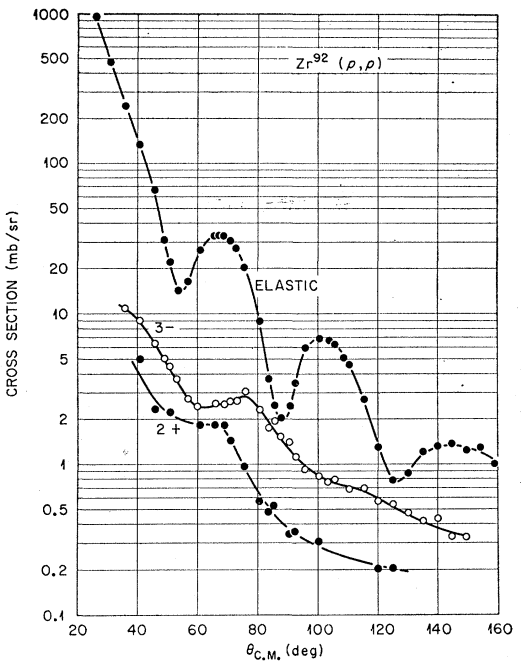

FIG. 2. Angular distributions of elastic and inelastic scattering to low-lying levels in Zr^{92}. The solid lines are drawn to emphasize the features of the data.

RESULTS

A typical angular distribution is shown in Fig. 2. The angular distribution for the 2+ and 3− collective states is also shown to indicate the relative magnitudes of the cross sections. The small cross section observed for the 2+ collective state is in agreement with the assumption of a small deformation parameter. This conclusion is also supported by results from Coulomb excitation studies.[10]

The measured cross sections for the elastic scattering from the five zirconium isotopes are given in Table II. Only the Zr^{96} cross sections have been corrected for the isotopic impurities in the target. For the remaining isotopes, the purity of the principal isotope was good

[10] P. H. Stelson, in *Proceedings of the International Conference on Nuclear Structure* (University of Toronto Press, Toronto, 1960). p. 787.

TABLE II. Differential cross section for proton elastic scattering at 22.5 MeV.

$\theta_{c.m.}$ (deg)	Zr^{90} $\sigma(\theta)$ (mb/sr)	Zr^{91} $\sigma(\theta)$ (mb/sr)	Zr^{92} $\sigma(\theta)$ (mb/sr)	Zr^{94} $\sigma(\theta)$ (mb/sr)	Zr^{96} $\sigma(\theta)$ (mb/sr)
17.1	5240.	5220.		5710.	5750.
21.7	2150.	2200.	2250.	2380.	2470.
26.5	1040.	1050.	962.	1060.	1020.
28.4		767.		745.	
31.3	507.	488.	470.	457.	477.
33.2		391.		357.	
36.2	272.	274.	242.	243.	254.
38.1		223.		191.	
41.1	152.	146.	133.	131.	123.
43.0				92.6	
46.0	60.9	62.7	65.3	53.1	52.8
48.0	39.0				37.3
49.0		29.5	30.8	29.4	
51.0	19.6	19.5	21.9	20.2	20.6
52.9		14.2	14.2	16.0	
53.9	10.3				19.3
55.9	10.8	14.9		17.4	23.7
56.9			16.4		
57.9	14.2	17.0		21.8	
60.9	20.4	25.1	26.4	29.3	37.8
65.8	32.1	33.6	32.5	35.7	39.9
68.8	32.9	34.5	32.5	33.4	34.5
70.8	30.9	31.1	29.9	28.1	29.0
72.8	26.4	26.4	27.0	22.1	22.5
75.8	19.9	21.5	20.3	15.4	12.1
80.7	9.36	8.46	8.93	5.76	4.23
83.7		3.96	3.63	2.75	
85.7	2.82	3.36	2.43	1.79	2.36
86.7	2.61				
87.7		2.20	1.98	2.15	
88.7	2.01				
90.6	2.03	2.32	2.41	3.05	4.54
92.6	2.65	3.16	3.40	4.12	
95.6	3.95	4.59	5.93	5.97	7.26
98.5				6.74	
100.5	6.01	6.45	6.76	7.07	8.04
103.5	6.08	6.50	6.56	6.70	7.47
105.5	6.49	6.43	6.24	5.80	5.82
107.4	6.09				
108.4		5.27	5.01	4.53	
110.4	4.26	4.95	4.57	3.48	3.88
115.3	2.64	2.73	2.65	1.86	1.21
120.2	1.43	1.63	1.25	0.82	0.60
125.1	1.03	1.10	0.77	0.78	0.75
130.0	0.97	1.25	0.86	1.02	1.62
134.9	1.08	1.31	1.19	1.32	2.06
139.7	1.23	1.57	1.28	1.37	1.84
144.6	1.40	1.44	1.33	1.27	1.46
149.4	1.62	1.56	1.20	1.20	1.19
154.1	1.91	1.52	1.26	0.91	0.78
158.8		0.54	0.98	0.92	

enough or the isotopic impurities were distributed such that the measured cross sections were effectively unchanged. Absolute errors in the measured cross sections are estimated at $\pm 10\%$. The largest part of this error is attributed to the nonuniformity of the target foils.

A plot of all of the angular distributions, as ratio-to-Rutherford, is shown in Fig. 3. A smooth change in the angular features of the distributions is observed from isotope to isotope. The positions of the maxima and minima as a function of $A^{-1/3}$ are plotted in Fig. 4. A similar plot is given in Ref. 6 for nuclei over a wide range of A values. A comparison of the two figures shows that the angular features of the zirconium distributions exhibit a larger shift in position than would have been expected from the average behavior of nuclei in this region of mass. This is qualitatively in agreement with the presence of a nuclear symmetry term in the optical-model real potential.

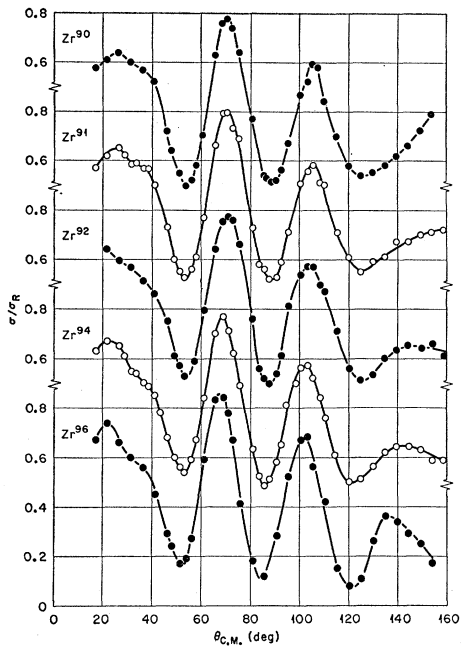

FIG. 3. Proton elastic scattering for the five stable zirconium isotopes, plotted as ratio-to-Rutherford scattering. The solid lines serve only to connect the experimental points. The cross sections of Table II have been reduced 5% for ease of comparison with Fig. 6.

ANALYSIS

Optical-model calculations were performed with the ORNL automatic search code HUNTER,[11] which minimizes the quantity

$$\chi^2=\sum_i \frac{|\sigma_{\rm th}(\theta_i)-\sigma_{\rm ex}(\theta_i)|^2}{\Delta\sigma^2}.$$

Details of the operation of this code can be found in a survey of deuteron elastic scattering.[12] The potential assumed for the real well is of the standard Saxon shape

$$V(r)=V/(1+e^x),$$
$$x=(r-R_0)/a,$$
$$R_0=r_0A^{1/3},$$

where V is the real well strength. The quantities r_0 and a are the geometrical parameters. The imaginary well is taken as a mixture of volume absorption and

[11] R. M. Drisko (unpublished).
[12] E. C. Halbert, Nucl. Phys. **50**, 353 (1964).

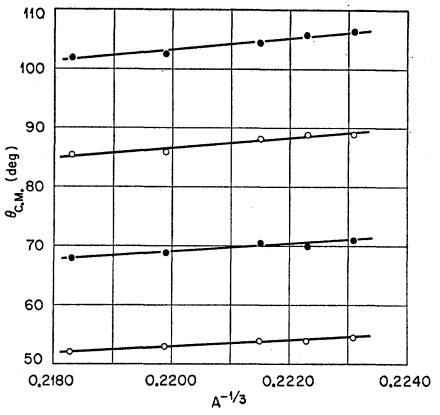

FIG. 4. Maxima and minima of experimental angular distributions, plotted as a function of $A^{-1/3}$.

surface absorption,

$$W(r)=W/(1+e^{x'})+[4W'e^{x'}/(1+e^{x'})^2],$$

where $x'=(r-R_w)/a_w$, $R_w=r_wA^{1/3}$, and W and W' are the coefficients of the volume and surface absorption wells, respectively. The charge interaction is taken of the form

$$V_C=Ze^2/r, \quad r\geq R_0,$$

and

$$V_C=(Ze^2/2R_0)(3-r^2/R_0^2), \quad r\leq R_0,$$

and the spin-orbit interaction is of the Thomas type,

$$V_s(r)=(\sigma\cdot l)(2V_s/rV)[dV(r)/dr].$$

In our calculations most attention was paid to the

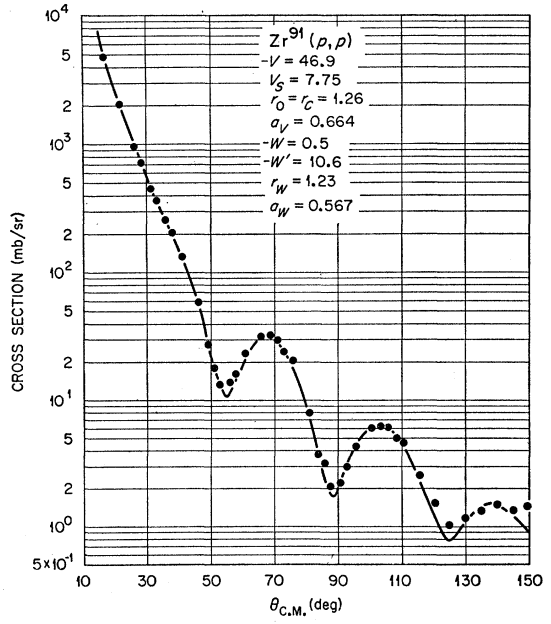

FIG. 5. Fixed geometry theoretical angular distribution compared with experiment.

TABLE III. Optical-model parameters.

Quantity	Value
Volume imaginary potential, W	−0.5 MeV
Radius parameter for real potential, r_0	1.26 F
Diffusivity parameter for real potential, a	0.664 F
Surface imaginary potential, W'	−10.6 MeV
Radius parameter for imaginary potentials, r_w	1.23 F
Diffusivity parameter for imaginary potentials, a_w	0.567 F
Spin-orbit potential, V_s	7.75 MeV

data in the angular range from 30 to 120°, where the measured cross sections are considered to be least subject to systematic errors. The procedure followed was to use the parameters found by Perey[7] for the initial guess parameters in the search code. After optimum fits to the data were found, an average set of real and

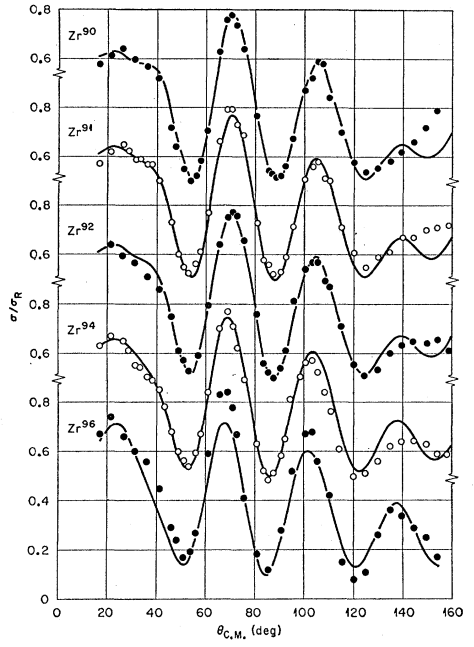

FIG. 6. Proton elastic scattering for the five stable zirconium isotopes, plotted as ratio-to-Rutherford scattering. The solid lines are the theoretical fit to the experimental points. The cross sections listed in Table II have been reduced by 5%. This change is within the experimental uncertainty and was done on the basis of subjectivity improving the over-all theoretical fits.

imaginary well geometrical parameters and imaginary well strength parameters were chosen. These parameters are listed in Table III. The search code was then allowed to vary the real well depth V_0 until an optimum fit was found under these restricted conditions. A typical fit for these parameters is shown in Fig. 5.

The quality of the fits is emphasized by plotting the ratio of the cross sections to the Rutherford cross section; these curves for the parameters of Table III are shown in Fig. 6 for the five isotopes.

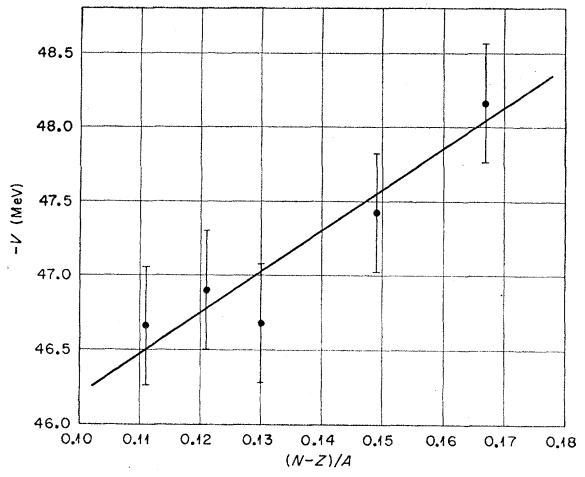

FIG. 7. Real nuclear potential depth V, plotted as a function of $(N-Z)/A$. The line is a least squares straight line fit to the results of the optical-model search and has a slope of 27.8±6.0 MeV.

The best-fit values of real nuclear potential depth V are plotted as a function of $(N-Z)/A$ in Fig. 7. The limits of uncertainty on V were set on the basis of the change in V necessary to shift the positions of maxima and minima beyond the experimental uncertainty in angle. A straight-line least-squares fit to these points yields a value of $V_0=-43.4\pm0.8$ MeV and $V_1=27.8\pm6.0$ MeV [see Eq. (2)]. This value does not include any Coulomb correction.

DISCUSSION

The values we have quoted for the real potential strengths implicitly include a Coulomb correction, which correction is not uniquely known. If we assume the form taken by Perey,[7]

$$V'_C=0.4Z/A^{1/3},$$

the symmetry potential depth is increased about 1 MeV. Since the application of the correction is somewhat arbitrary in the case of isotopes and since the magnitude of the effect is well within our estimated errors, the correction is omitted.

The magnitude of the symmetry term of the nuclear potential found in this work is in good agreement with the range of values summarized by Hodgson,[13] and with estimates deduced from (p,n) reactions.[14] Comparison of the results of this analysis with Perey's analysis of lower energy data shows no evidence that the magnitude of the symmetry potential is velocity dependent.

No evidence is seen for an effect of the closed neutron shell in Zr^{90} on the optical-model parameters.

ACKNOWLEDGMENTS

We are indebted to G. R. Satchler and R. M. Drisko for helpful discussions.

[13] P. E. Hodgson, Phys. Letters 3, 352 (1963).
[14] R. M. Drisko, R. H. Bassel, and G. R. Satchler, Phys. Letters 2, 318 (1962).